

Three-body interaction near a narrow two-body zero crossing

A. Pricoupenko and D. S. Petrov

LPTMS, CNRS, Univ. Paris-Sud, Université Paris-Saclay, F-91405 Orsay, France

(Dated: October 31, 2021)

We calculate the effective three-body force for bosons interacting with each other by a two-body potential tuned to a narrow zero crossing in any dimension. We use the standard two-channel model parametrized by the background atom-atom interaction strength, the amplitude of the open-channel to closed-channel coupling, and the atom-dimer interaction strength. The three-body force originates from the atom-dimer interaction, but it can be dramatically enhanced for narrow crossings, i.e., for small atom-dimer conversion amplitudes. This effect can be used to stabilize quasi-two-dimensional dipolar atoms and molecules.

PACS numbers:

I. INTRODUCTION

In recent years, dilute weakly interacting bosons with intentionally weakened mean-field interactions have become one of the main attractions in the field of quantum gases. The weakness of the mean-field interaction in such systems makes higher-order terms relatively more important leading to dramatic effects. A prominent example is the observation of dilute quantum droplets in dipolar atoms [1–4] and in nondipolar mixtures [5–7]. Two-body interactions of different kinds (contact and dipole-dipole in the dipolar case and interspecies and intraspecies in the mixture case) are tuned to compete with each other such that the resulting weak overall attraction gets compensated by a higher-order Lee-Huang-Yang (LHY) term [8–10]. An impressive experimental progress has been made in the dipolar case on pursuing supersolidity through the formation of coherent arrays of quantum droplets [11–15].

All these achievements correspond to essentially three-dimensional setups well described by the Gross-Pitaevskii energy density functional with an additional local LHY term $\propto n^{5/2}$, where n is the density. However, there are various reasons to consider other configurations where the $n^{5/2}$ term is absent or too weak (low-dimensional geometries, single-component contact-interacting atoms, etc.) In these cases, an effective three-body interaction, associated with a n^3 term in the energy density, can become dominant if the leading-order two-body forces are suppressed. In particular, three-body forces have been considered in the context of droplet formation in three dimensions [16–19] and as a means for stabilizing supersolid phases of quasi-two-dimensional dipolar atoms or molecules [20]. Quite a few recent theory papers have discussed one-dimensional three-body-interacting systems, exploring the kinematic equivalence of the three-body scattering in one dimension and the two-body scattering in two dimensions (see, for example, Refs. [21–32]).

In this paper we analyze a simple mechanism for the emergence of an effective three-body interaction. Namely, we consider bosons interacting with each other by a potential tuned to a zero crossing near a narrow Feshbach resonance, where the conversion amplitude from

atoms to closed-channel dimers is small and where the two-body scattering amplitude is characterized by a large effective range R_e . The effective three-body force appears in this model when one takes into account the interaction between atoms and closed-channel dimers, characterized by the coupling strength g_{12} . We find that the three-body coupling constant g_3 in D dimensions is proportional to $R_e^D g_{12}$ and can thus be enhanced near narrow two-body zero crossings.

The paper is organized as follows. In Sec. II we introduce the two-channel model and perform its mean-field analysis. In the dilute limit the density of closed-channel dimers in the system scales as $R_e^D n^2 \ll n$ and the effective three-body interaction emerges simply as the atom-dimer mean-field interaction energy $\propto R_e^D g_{12} n^3$. We show that this simple mechanism, applied to two-dimensional dipoles, generates conditions for observing supersolid phases predicted in Ref. [20].

In Secs. III and IV we turn to the few-body perspective and perform a detailed nonperturbative analysis of the two-body (Sec. III) and three-body (Sec. IV) problems with zero-range potentials. In particular, the three-body scattering length near a narrow two-body zero crossing is found for an arbitrary atom-dimer interaction strength in any dimension.

II. MEAN-FIELD ANALYSIS

We start with the two-channel model described by the Hamiltonian [33]

$$\hat{H} = \int_{\mathbf{r}} \left\{ -\hat{\psi}_1^\dagger(\mathbf{r}) \frac{\nabla^2}{2} \hat{\psi}_1(\mathbf{r}) + \hat{\psi}_2^\dagger(\mathbf{r}) \left(-\frac{\nabla^2}{4} + \nu_0 \right) \hat{\psi}_2(\mathbf{r}) - \frac{\alpha}{2} [\hat{\psi}_1^\dagger(\mathbf{r}) \hat{\psi}_1^\dagger(\mathbf{r}) \hat{\psi}_2(\mathbf{r}) + \text{h.c.}] + \sum_{\sigma\sigma'} \frac{g_{\sigma\sigma'}}{2} \hat{n}_\sigma(\mathbf{r}) \hat{n}_{\sigma'}(\mathbf{r}) \right\}, \quad (1)$$

where $\hat{\psi}_1$ and $\hat{\psi}_2$ are, respectively, the annihilation operators of atoms and dimers, \hat{n}_σ are the corresponding density operators, ν_0 is the detuning parameter, $g_{\sigma\sigma'}$ are interaction constants, α is the atom-dimer conversion amplitude (without loss of generality assumed real

and positive), and we have set \hbar and atom mass equal to 1. Hereafter, $\int_{\mathbf{r}}$ denotes $\int d^D r$.

In the mean-field description of (1) we assume pure atomic and molecular condensates $\hat{\psi}_\sigma = \sqrt{n_\sigma}$ with the same phase (which corresponds to the energy minimum for $\alpha > 0$) [33]. We arrive at the energy density

$$E/L^D = \nu_0 n_2 - \alpha n_1 \sqrt{n_2} + \sum_{\sigma\sigma'} g_{\sigma\sigma'} n_\sigma n_{\sigma'}/2, \quad (2)$$

which we minimize with respect to n_2 (or n_1) keeping the total density $n = n_1 + 2n_2$ constant. For positive ν_0 and small n the dimer population behaves quadratically in n

$$n_2 = \left(\frac{\alpha n}{2\nu_0}\right)^2 \left(1 + \frac{4g_{11}\nu_0 - 2g_{12}\nu_0 - 3\alpha^2}{\nu_0^2} n\right) + O(n^4) \quad (3)$$

and the energy density reads

$$\frac{E}{L^D} = \left(\frac{g_{11}}{2} - \frac{\alpha^2}{4\nu_0}\right) \left(n^2 - \frac{\alpha^2}{\nu_0^2} n^3\right) + \frac{g_{12}\alpha^2}{4\nu_0^2} n^3 + O(n^4). \quad (4)$$

The two-body zero crossing occurs at the detuning $\nu_0 = \alpha^2/2g_{11}$ where the first term in the right-hand side of Eq. (4) vanishes. One can then see that the residual three-body energy shift originates from the direct mean-field interaction of atoms with dimers. It equals $g_{12}n_1n_2 \approx g_3n^3/3!$ with

$$g_3 = 6g_{12}g_{11}^2/\alpha^2 = 3g_{12}R_e^D. \quad (5)$$

The effective volume $R_e^D = 2g_{11}^2/\alpha^2$ introduced in Eq. (5) characterizes the closed-channel population. Indeed, the density of dimers can be written as

$$n_2 \approx R_e^D n^2/2 \quad (6)$$

meaning that each pair of atoms is found in the closed-channel dimer state with probability $(R_e/L)^D$.

If $g_{\sigma\sigma'}$ are of the same order of magnitude $\sim g$, the expansion (4) is in powers of $R_e^D n$, which we assume small. Then, at the zero crossing the three-body term gives the leading contribution to the energy density $\sim gn^2(R_e^D n)^1$ and we neglect subleading terms such as, for instance, the dimer-dimer interaction $\sim g_{22}\alpha^4 n^4/\nu_0^4 \sim gn^2(R_e^D n)^2$. On the other hand, it may be interesting to keep a small but finite effective two-body interaction $g_{\text{eff}} = g_{11} - \alpha^2/2\nu_0 \sim g(R_e^D n) \ll g$, so that it can compete with the three-body term. It is also useful to note that the effective two-body interaction depends on the collisional momentum as $g_{\text{eff}}(k) = g_{\text{eff}}(0) - R_e^D k^2$ (see [35] and Sec. III). However, if $k \ll \sqrt{gn}$, the corresponding effective-range correction gives a contribution to (4) much smaller than $gn^2(R_e^D n)^1$. We thus conclude that on this level of expansion we reduce (1) to the model of scalar bosons with local effective two-body and three-body interactions.

A. Application to two-dimensional dipoles

Having in mind supersolid phases, which require a three-body repulsive force [20], let us perform the same mean-field analysis in the case of two-dimensional dipoles oriented perpendicular to the plane. Instead of pointlike interactions characterized by the momentum-independent constants $g_{\sigma\sigma'}$ we now assume momentum-dependent pseudopotentials [20, 34]

$$\tilde{V}_{\sigma\sigma'}(|\mathbf{k} - \mathbf{k}'|) = g_{\sigma\sigma'} - 2\pi d_\sigma d_{\sigma'} |\mathbf{k} - \mathbf{k}'|, \quad (7)$$

where \mathbf{k} and \mathbf{k}' are the incoming and outgoing relative momenta and d_1 and d_2 are dipole moments of atoms and dimers, respectively. The pseudopotential (7) is an effective potential valid only for the leading-order mean-field analysis at low momenta. Its coordinate representation

$$V_{\sigma\sigma'}(\mathbf{r} - \mathbf{r}') = \int \frac{d^2 q}{(2\pi)^2} \tilde{V}_{\sigma\sigma'}(q) e^{i\mathbf{q}(\mathbf{r} - \mathbf{r}')} \quad (8)$$

has the long-distance asymptote $d_\sigma d_{\sigma'}/r^3$ with the characteristic range $r_{\sigma\sigma'}^* = 2\mu_{\sigma\sigma'} d_\sigma d_{\sigma'}$, where $\mu_{11} = 1/2$ and $\mu_{12} = 2/3$ are the atom-atom and atom-dimer reduced masses, respectively.

Obviously, for homogeneous condensates the momentum-dependent part of (7) plays no role and our previous analysis holds. Namely, we arrive at the energy density $E/L^2 = g_{\text{eff}} n^2/2 + g_3 n^3/6$, where $g_{\text{eff}} = g_{11} - \alpha^2/2\nu_0$ is tuned to be small and g_3 is given by Eq. (5). Let us now assume that the atomic and dimer condensates are spatially modulated with a characteristic momentum k (in the supersolid phase the modulation is periodic). Then, the most important new terms in Eqs. (2) and (4) are the kinetic energy of the atomic component $\sim nk^2$ and the momentum-dependent part of the atom-atom interaction $\sim -r_{11}^* kn^2$. Minimizing their sum with respect to k gives a contribution $\epsilon_{\text{mod}} \sim -r_{11}^{*2} n^3$ to the energy density and the optimal modulation momentum $k_{\text{min}} \sim r_{11}^* n$ [20]. One can check that other momentum-dependent terms are subleading. For instance, the kinetic energy of dimers $\sim n_2 k^2$ and the momentum-dependent atom-dimer interaction $\sim r_{12}^* knn_2$ carry an additional factor $R_e^D n \ll 1$. It is important to mention that the density of dimers satisfies Eq. (6) locally, i.e., $n_2(\mathbf{r}) \approx R_e^D n^2(\mathbf{r})/2$. Deviations from this relation, which follows from minimizing the first two terms in the right-hand side of Eq. (2), are energetically too costly. A change of n_2 by, say, a factor of two compared to the optimal value would cost $\sim g_{11} n^2 \gg gn^2(R_e^D n)$ in the energy density.

This analysis leads us to the model of two-dimensional dipoles characterized by an effective two-body pseudopotential $\tilde{V}(k) = g_{\text{eff}} - 2\pi d_1^2 k$ and local three-body term $g_3 \delta(\mathbf{r}_1 - \mathbf{r}_2) \delta(\mathbf{r}_2 - \mathbf{r}_3)$. The mean-field phase diagram of this model has been worked out in Ref. [20]. It has been shown that the stability of the system with respect to collapse is ensured by the repulsive three-body interaction term compensating the effectively attractive ϵ_{mod} , which

also scales as n^3 . The supersolid stripe, honeycomb and triangular phases are predicted when these two terms are comparable and $g_{\text{eff}} < 0$. To give a concrete example, the four-critical point where the three supersolid phases meet with one another and with the uniform phase (this is also the point where the roton minimum touches zero) is characterized by $g_{12}R_e^2 = 2(\pi r_{11}^*)^2$ and $nR_e^2 = |g_{\text{eff}}|/g_{12}$.

B. Inelastic losses

Collisions of atoms with closed-channel dimers can lead to the relaxation to more deeply bound molecular states. The rate of this process in a unit volume is given by $\alpha_r n_1 n_2$, where α_r is the relaxation rate constant. In our model this corresponds to the atom loss rate $\dot{n} = -(3/2)\alpha_r R_e^D n^3$, and we see that this effective three-body loss gets enhanced with increasing R_e in the same manner as the elastic three-body interaction (5). In fact, the atom-dimer relaxation can be mathematically modeled by allowing g_{12} to be complex. Shotan and co-workers [35] have measured the three-body loss rate constant near a two-body zero crossing in three dimensions. They argue that this quantity is proportional to R_e^4 . Here we claim a slightly different scaling ($\propto R_e^3$), valid when R_e is much larger than the van der Waals range.

For Feshbach molecules of the size of the van der Waals length α_r is typically of the same order of magnitude as g_{12} . The lifetime of the sample is thus comparable to the timescale associated with the elastic three-body energy shift. There are, however, ways of overcoming this problem. For dipoles oriented perpendicular to the plane in the quasi-two-dimensional geometry inelastic processes are suppressed by the predominantly repulsive dipolar tail. For instance, for Dy the atom-dimer dipolar length r_{12}^* can reach about 50 nm depending on the magnetic moment of the closed-channel dimer. The confinement of frequency $\omega = 2\pi \times 100$ kHz for this system gives the oscillator length $\sqrt{\hbar/2\mu_{12}\omega} \approx 21$ nm. Under these conditions one expects a noticeable reduction of the relaxation rate [36–38]. This mechanism may work also for dipolar molecules where larger values of r_{12}^* can be reached.

A different approach to this problem is to consider closed-channel dimers which are weakly-bound and have a halo character, i.e., well extended beyond the support of the potential. A specific way of generating three-body interactions in this manner has been proposed by one of us in Ref. [17]; two atoms in state 1 collide and both go to another internal state 1' where they form an extended molecular state. The effective three-body force is then due to a repulsive mean-field interaction between atoms 1' and a third atom in state 1. In this case, the relaxation is slow since the dimer is not “preformed”.

III. REGULARIZED MODEL AND TWO-BODY PROBLEM

We now go back to the model (1), try to analyze it from the few-body viewpoint, and characterize the three-body interaction beyond the mean-field result (5) (also trying to determine its validity regime). Clearly, at some point the strength of the background atom-atom interaction becomes a relevant parameter (not just the ratio g_{11}/α). One also observes that the pointlike interaction and conversion terms in Eq. (1) lead to divergences and have to be regularized in dimensions $D > 1$, which necessitates an additional parameter (a short-range or high-momentum cutoff).

In order to regularize the model (1) we use the delta-shell pseudopotential representation [39, 40] with a finite range r_0 . Namely, we rewrite Eq. (1) as

$$\begin{aligned} \hat{H} = & \int_{\mathbf{r}} -\hat{\psi}_1^\dagger(\mathbf{r}) \frac{\nabla^2}{2} \hat{\psi}_1(\mathbf{r}) + \hat{\psi}_2^\dagger(\mathbf{r}) \left(-\frac{\nabla^2}{4} + \nu_0 \right) \hat{\psi}_2(\mathbf{r}) \\ & + \sum_{\sigma\sigma'} \frac{g_{\sigma\sigma'}}{2} \int_{\mathbf{r}} \int_{\mathbf{y}} \tilde{\delta}_{r_0}(\mathbf{y}) \hat{n}_\sigma(\mathbf{r} + \mathbf{y}/2) \hat{n}_{\sigma'}(\mathbf{r} - \mathbf{y}/2) \\ & - \frac{\alpha}{2} \int_{\mathbf{r}} \int_{\mathbf{y}} \tilde{\delta}_{r_0}(\mathbf{y}) [\hat{\psi}_1^\dagger(\mathbf{r} + \mathbf{y}/2) \hat{\psi}_1^\dagger(\mathbf{r} - \mathbf{y}/2) \hat{\psi}_2(\mathbf{r}) + \text{h.c.}], \end{aligned} \quad (9)$$

where $\tilde{\delta}_{r_0}(\mathbf{y}) = \delta(|\mathbf{y}| - r_0)/S_D(r_0)$ is the normalized delta shell with $S_1(r_0) = 2$, $S_2(r_0) = 2\pi r_0$, and $S_3(r_0) = 4\pi r_0^2$. The range r_0 should be understood as the smallest lengthscale in our problem. It does not enter in the final formulas and it is just a convenient way to regularize the problem without using zero-range pseudopotentials, which have different forms in different dimensions. In the one-dimensional case r_0 can be set to zero from the very beginning, but we keep it finite in order to use the same formalism for the cases with different D . Note also that we do not intend to consider effects of scattering with angular momenta $l \neq 0$. This is to say that, as r_0 is decreased, the coupling constants $g_{\sigma\sigma'}$ and α are tuned to reproduce desired (physical) R_e and $a_{\sigma\sigma'}$ only for the s -wave channel. Then, in the limit $r_0 \rightarrow 0$, the terms $g_{\sigma\sigma'}\tilde{\delta}_{r_0}(\mathbf{y})$ and $\alpha\tilde{\delta}_{r_0}(\mathbf{y})$ are too weak to induce any scattering for $l > 0$.

A stationary two-body state with zero center-of-mass momentum and $l = 0$ in the two-channel models (1) or (9) is represented by

$$\int_{\mathbf{c}} \int_{\mathbf{y}} \Psi(\mathbf{y}) \hat{\psi}_1^\dagger(\mathbf{c} + \mathbf{y}/2) \hat{\psi}_1^\dagger(\mathbf{c} - \mathbf{y}/2) |0\rangle + \int_{\mathbf{c}} \phi \hat{\psi}_2^\dagger(\mathbf{c}) |0\rangle, \quad (10)$$

where $|0\rangle$ is the vacuum state. Acting on (10) by the operator $\hat{H} - E$, and requiring that the result vanish, we get the coupled Schrödinger equations at energy E ,

$$[-\nabla_{\mathbf{y}}^2 - E + g_{11}\tilde{\delta}_{r_0}(\mathbf{y})]\Psi(\mathbf{y}) = \alpha\tilde{\delta}_{r_0}(\mathbf{y})\phi/2, \quad (11)$$

$$(\nu_0 - E)\phi = \alpha\Psi(r_0), \quad (12)$$

which, upon eliminating the closed-channel amplitude ϕ , become

$$[-\nabla_{\mathbf{y}}^2 - E + g_{\text{eff}}(E)\tilde{\delta}_{r_0}(y)]\Psi(y) = 0 \quad (13)$$

with

$$g_{\text{eff}}(E) = g_{11} + \frac{1}{2} \frac{\alpha^2}{E - \nu_0}. \quad (14)$$

The zero crossing condition at zero energy thus reads

$$\nu_0 = \alpha^2/2g_{11}. \quad (15)$$

We also introduce the effective range by the formula

$$R_e^D = \alpha^2/2\nu_0^2 > 0, \quad (16)$$

which characterizes the small- E asymptote $g_{\text{eff}}(E) = g_{\text{eff}}(0) - R_e^D E + O(E^2)$ (cf. [35]). At the crossing Eq. (16) is consistent with our earlier definition of R_e introduced in Eq. (5). As we have mentioned, R_e^D is also related to the closed-channel occupation. Indeed, from the normalization integral of Eq. (10) one finds that the closed-channel to open-channel probability ratio equals $|\phi|^2/\int_{\mathbf{y}} 2|\Psi(y)|^2 = |\phi|^2/(2L^D|\Psi(r_0)|^2)$ where we have used the fact that at the crossing $\Psi(y) = \Psi(r_0)$. On the other hand, from Eq. (12) one obtains $|\phi|^2 = 2R_e^D|\Psi(r_0)|^2$ for $|E| \ll |\nu_0|$, which gives the result claimed in Sec. II. Namely, the probability for two atoms to be in the closed-channel dimer state equals $(R_e/L)^D$.

Eventually, we will need to express our results in terms of the scattering lengths $a_{\sigma\sigma'}$ and the effective range R_e rather than in terms of the bare r_0 -dependent quantities $g_{\sigma\sigma'}$, α , and ν_0 . Relations between $g_{\sigma\sigma'}$ and $a_{\sigma\sigma'}$ are obtained by solving the scattering problem at zero collision energy and by looking at the long-distance asymptote of the two-body wave function. Namely, the zero-energy Schrödinger equation reads

$$[-\nabla_{\mathbf{y}}^2 + 2\mu_{\sigma\sigma'}g_{\sigma\sigma'}\tilde{\delta}_{r_0}(y)]\Psi(y) = 0. \quad (17)$$

In one dimension the (unnormalized) solution is

$$\Psi(y) = \begin{cases} 1, & |y| < r_0 \\ 1 + \mu_{\sigma\sigma'}g_{\sigma\sigma'}(|y| - r_0), & |y| > r_0, \end{cases} \quad (18)$$

from which we see that

$$a_{\sigma\sigma'} = r_0 - 1/\mu_{\sigma\sigma'}g_{\sigma\sigma'}. \quad (19)$$

In the limit $r_0 \rightarrow 0$ we recover the usual relation $g_{\sigma\sigma'} = -1/\mu_{\sigma\sigma'}a_{\sigma\sigma'}$. In two dimensions the solution of Eq. (17) reads

$$\Psi(\mathbf{y}) = \begin{cases} 1, & |\mathbf{y}| < r_0 \\ 1 + \mu_{\sigma\sigma'}g_{\sigma\sigma'} \ln(|\mathbf{y}|/r_0)/\pi, & |\mathbf{y}| > r_0 \end{cases} \quad (20)$$

and one has

$$\mu_{\sigma\sigma'}g_{\sigma\sigma'} = \pi/\ln(r_0/a_{\sigma\sigma'}). \quad (21)$$

In three dimensions

$$\Psi(\mathbf{y}) = \begin{cases} 1, & |\mathbf{y}| < r_0 \\ 1 - \mu_{\sigma\sigma'}g_{\sigma\sigma'}/2\pi|\mathbf{y}| + \mu_{\sigma\sigma'}g_{\sigma\sigma'}/2\pi r_0, & |\mathbf{y}| > r_0, \end{cases} \quad (22)$$

from which we obtain

$$1/a_{\sigma\sigma'} = 2\pi/\mu_{\sigma\sigma'}g_{\sigma\sigma'} + 1/r_0. \quad (23)$$

We now analyze conditions for having two-body bound states at the two-body zero crossing, in particular, having in mind the three-body recombination to these states when considering the three-body problem. We just note that solutions of Eq. (13) at distances $|y| \ll 1/\sqrt{|E|}$ in different dimensions are given, respectively, by Eqs. (18), (20), and (22) with $\sigma = \sigma' = 1$ and with g_{11} substituted by $g_{\text{eff}}(E)$. We then match these asymptotes with the decaying solutions $\Psi^{(D=1)}(y) \propto \exp(\kappa|y|)$, $\Psi^{(D=2)}(y) \propto K_0(\kappa|\mathbf{y}|)$, and $\Psi^{(D=3)}(y) \propto \exp(-\kappa|\mathbf{y}|)/|\mathbf{y}|$, where $\kappa = \sqrt{-E}$. This matching procedure gives the following equations for the determination of κ ($\gamma \approx 0.577$ is the Euler constant):

$$(\kappa R_e)^2(a_{11}/R_e) - \kappa R_e = 2, \quad D = 1, \quad (24)$$

$$(\kappa R_e)^2 \ln(\kappa a_{11} e^\gamma/2) = 2\pi, \quad D = 2, \quad (25)$$

$$(\kappa R_e)^3 - (\kappa R_e)^2(R_e/a_{11}) = 4\pi, \quad D = 3. \quad (26)$$

Analyzing these equations we find that in one dimension there is no two-body bound state, if $a_{11} < 0$ (or $g_{11} > 0$). In higher dimensions we always have a bound state, but it becomes deep in the limit of small positive a_{11} ($E \propto -1/a_{11}^2$). In principle, the case of a weak repulsive background atom-atom interaction can also be realized by a finite-range repulsive potential (in the mean-field spirit of Sec. II). Then, the dimer states given by Eqs. (24-26) are spurious, consistent with the fact that the zero-range theory can no longer be used at such high momenta.

IV. THREE-BODY PROBLEM

Similar to Eq. (10) a stationary state of three atoms with zero center-of-mass momentum can be written in the form

$$\int_{\mathbf{c}} \int_{\mathbf{x}} \int_{\mathbf{y}} \Psi(\mathbf{x}, \mathbf{y}) \hat{\psi}_1^\dagger(\mathbf{c} - \mathbf{x}/2\sqrt{3} - \mathbf{y}/2) \hat{\psi}_1^\dagger(\mathbf{c} - \mathbf{x}/2\sqrt{3} + \mathbf{y}/2) \hat{\psi}_1^\dagger(\mathbf{c} + \mathbf{x}/\sqrt{3}) |0\rangle + \int_{\mathbf{c}} \int_{\mathbf{x}} \phi(\mathbf{x}) \hat{\psi}_2^\dagger(\mathbf{c} - \mathbf{x}/2\sqrt{3}) \hat{\psi}_1^\dagger(\mathbf{c} + \mathbf{x}/\sqrt{3}) |0\rangle, \quad (27)$$

where \mathbf{c} is the center-of-mass coordinate and the relative Jacobi coordinates are

$$\begin{aligned} \mathbf{x} &= (2\mathbf{r}_1 - \mathbf{r}_2 - \mathbf{r}_3)/\sqrt{3}, \\ \mathbf{y} &= \mathbf{r}_3 - \mathbf{r}_2. \end{aligned} \quad (28)$$

Let us introduce operators \hat{P}_+ and \hat{P}_- which exchange the first atom with the second and the third, respec-

tively. Acting by these operators on an arbitrary function $F(\mathbf{x}, \mathbf{y})$ results in

$$\hat{P}_\pm F(\mathbf{x}, \mathbf{y}) = F(-\mathbf{x}/2 \mp \sqrt{3}\mathbf{y}/2, -\sqrt{3}\mathbf{x}/2 \pm \mathbf{y}/2). \quad (29)$$

The open-channel wave function $\Psi(\mathbf{x}, \mathbf{y})$ is invariant with respect to these permutations.

The coupled Schrödinger equations for Ψ and ϕ read

$$[-\nabla_{\mathbf{x}}^2 - \nabla_{\mathbf{y}}^2 - E + g_{11}(1 + \hat{P}_+ + \hat{P}_-)\tilde{\delta}_{r_0}(y)]\Psi(\mathbf{x}, \mathbf{y}) = \alpha(1 + \hat{P}_+ + \hat{P}_-)\tilde{\delta}_{r_0}(y)\phi(\mathbf{x})/2, \quad (30)$$

$$[-\nabla_{\mathbf{x}}^2 - \nu_0 - E + g_{12}\tilde{\delta}_{r_0}(\sqrt{3}x/2)]\phi(\mathbf{x}) = \alpha\Psi(\mathbf{x}, r_0), \quad (31)$$

where $\Psi(\mathbf{x}, r_0)$ in the right-hand side of Eq. (31) denotes the projection on the s -wave channel in the coordinate \mathbf{y} , i.e., the angular average $\langle \Psi(\mathbf{x}, r_0 \hat{y}) \rangle_{\hat{y}}$. The difference between $\Psi(\mathbf{x}, r_0 \hat{y})$ and $\Psi(\mathbf{x}, r_0)$, which accounts for non- s -wave scattering channels, vanishes in the limit $r_0 \rightarrow 0$ and we will thus make the replacement $\tilde{\delta}_{r_0}(y)\Psi(\mathbf{x}, \mathbf{y}) \rightarrow \tilde{\delta}_{r_0}(y)\Psi(\mathbf{x}, r_0)$ in Eq. (30). Then, it is convenient (the reason will become clear below) to introduce an auxiliary function $f(\mathbf{x})$ such that

$$\Psi(\mathbf{x}, r_0) = -f(\mathbf{x})/g_{11} + \alpha\phi(\mathbf{x})/2g_{11}. \quad (32)$$

We now eliminate Ψ from Eqs. (30) and (31) in favor of f and thus derive coupled equations for f and ϕ . To this end we note that with the use of (32) Eq. (30) becomes

$$(-\nabla_{\mathbf{x}}^2 - \nabla_{\mathbf{y}}^2 - E)\Psi(\mathbf{x}, \mathbf{y}) = (1 + \hat{P}_+ + \hat{P}_-)\tilde{\delta}_{r_0}(y)f(\mathbf{x}). \quad (33)$$

Equation (33) can now be solved with respect to Ψ by using the Green function $G_E^{(2D)}$ of the $2D$ -dimensional Helmholtz operator in the left-hand side (see, for example, Ref. [41]). This procedure gives

$$\Psi(\mathbf{x}, r_0) = \Psi_0(\mathbf{x}, 0) + \int_{\mathbf{x}'} \left\{ G_E^{(2D)}[\sqrt{(\mathbf{x} - \mathbf{x}')^2 + r_0^2}] + \sum_{\pm} G_E^{(2D)}(\sqrt{x^2 \pm \mathbf{x}\mathbf{x}' + x'^2}) \right\} f(\mathbf{x}'), \quad (34)$$

where $\Psi_0(\mathbf{x}, \mathbf{y})$ is any solution of $(-\nabla_{\mathbf{x}}^2 - \nabla_{\mathbf{y}}^2 - E)\Psi_0(\mathbf{x}, \mathbf{y}) = 0$. In Eq. (34) we have already taken the limit $r_0 \rightarrow 0$, where it exists. With the use of Eq. (34) the function $\Psi(\mathbf{x}, r_0)$ can now be eliminated from Eqs. (32) and (31). Here we explicitly write down the resulting coupled equations for f and ϕ at the two-body zero crossing ($\nu_0 = \alpha^2/2g_{11}$) and at zero energy ($E = 0$, $\Psi_0 = 1$):

$$\hat{L}f(\mathbf{x}) + f(\mathbf{x})/g_{11} = \phi(\mathbf{x})/\sqrt{2R_e^D} - 1, \quad (35)$$

$$[-\nabla_{\mathbf{x}}^2 + g_{12}\tilde{\delta}_{r_0}(\sqrt{3}x/2)]\phi(\mathbf{x}) = -\sqrt{2/R_e^D}f(\mathbf{x}), \quad (36)$$

where \hat{L} is the integral operator in the right-hand side of Eq. (34) with $E = 0$. We will use the following forms of

the zero-energy Green functions

$$G_0^{(2)}(\rho) = -\ln(\rho/R_e)/2\pi, \quad (37)$$

$$G_0^{(4)}(\rho) = 1/4\pi^2\rho^2, \quad (38)$$

$$G_0^{(6)}(\rho) = 1/4\pi^3\rho^4. \quad (39)$$

Equations (35) and (36) conserve angular momentum and parity. We will be interested in the case of positive parity (for $D = 1$) and zero angular momentum (for $D > 1$) so that $f(\mathbf{x}) = f(x)$ and $\phi(\mathbf{x}) = \phi(x)$. Note also that if $g_{12} = 0$, the solution of Eqs. (35) and (36) is $f(x) = 0$ and $\phi(x) = \sqrt{2R_e^D}$ indicating the absence of two-body and three-body interactions.

The quantity that we want to extract from solving Eqs. (35) and (36) is $\tilde{f}(0) = \int_{\mathbf{x}} f(x)$, which is proportional to the three-body scattering amplitude. Indeed, at large hyperradii $\rho = \sqrt{x^2 + y^2}$ Eq. (34) gives $\Psi \approx 1 + 3\tilde{f}(0)G_0^{(2D)}(\rho)$ or, explicitly,

$$\Psi = \begin{cases} 1 - 3\tilde{f}(0)\ln(\rho/R_e)/2\pi & \propto \ln(\rho/a_3), \quad D = 1, \\ 1 + 3\tilde{f}(0)/4\pi^2\rho^2 & \propto 1 - S_3/\rho^2, \quad D = 2, \\ 1 + 3\tilde{f}(0)/4\pi^3\rho^4 & \propto 1 - \Upsilon_3/\rho^4, \quad D = 3, \end{cases} \quad (40)$$

where we have introduced the three-body scattering length a_3 in one dimension, surface S_3 in two dimensions, and hypervolume Υ_3 in three dimensions:

$$a_3 = R_e \exp[2\pi/3\tilde{f}(0)], \quad D = 1, \quad (41)$$

$$S_3 = -3\tilde{f}(0)/4\pi^2, \quad D = 2, \quad (42)$$

$$\Upsilon_3 = -3\tilde{f}(0)/4\pi^3, \quad D = 3. \quad (43)$$

It is useful to note that for $D = 2, 3$ the three-body potential $g_3\delta(\sqrt{3}\mathbf{x}/2)\delta(\mathbf{y})$ with [42]

$$g_3 = -3(\sqrt{3}/2)^D \tilde{f}(0) \quad (44)$$

treated in the first Born approximation would produce the same scattered wave as Eqs. (40). Equations (42), (43), and (44) relate the three-body coupling constant g_3 to the three-body scattering surface and hypervolume. The corresponding contribution to the energy density of a three-body-interacting condensate equals $g_3 n^3/6$ in the weakly interacting regime, which is defined by $|S_3|n \ll 1$ in two dimensions and by $|\Upsilon_3|n^{4/3} \ll 1$ for $D = 3$. The quantity g_3/L^{2D} gives the energy shift for three (condensed) atoms in a large volume L^D . By solving the three-body problem nonperturbatively we calculate the exact g_3 , which can then be compared to the mean-field result given by Eq. (5).

The relation between a_3 and the three-body energy shift in the case $D = 1$ is slightly more subtle. Pastukhov [30] has recently shown that the ground-state energy density of a three-body-interacting one-dimensional Bose gas can be expanded in half-integer powers of the small parameter

$$g_3(n) = \sqrt{3}\pi/\ln(1/a_3 n) \ll 1, \quad (45)$$

with the leading-order term equal to $E/L = g_3(n)n^3/6$. Although, g_3 given by Eq. (45) depends on n , one can replace $1/n$ by another density-independent length scale l . If this scale is not exponentially different from $1/n$, the two small parameters are equivalent since they differ only by a higher-order term $\sim g_3^2$. By computing a_3 we

can thus compare Eqs. (5) and (45) which we expect to approach each other in the limit $R_e/a_{12} \rightarrow 0$ (at fixed n). Equivalently, one can say that in this limit Eq. (5) predicts the leading exponential dependence of the one-dimensional three-body scattering length

$$a_3 \propto \exp\left(\frac{\pi}{\sqrt{3}} \frac{\mu_{12} a_{12}}{R_e}\right) = \exp\left(\frac{2\pi}{3\sqrt{3}} \frac{a_{12}}{R_e}\right) \quad (46)$$

leaving, however, the preexponential factor unknown.

Returning to the task of determining $\tilde{f}(0)$ from Eqs. (35) and (36) we note that the three-body problem in hand admits a zero-range description parametrized by a_{11} , a_{12} , and R_e (see, however, Sec. IV C). Indeed, the sum $\hat{L}f(x) + f(x)/g_{11}$ in Eq. (35) is well behaved in the limit $r_0 \rightarrow 0$ since the singularity of $\hat{L}f(x)$ gets canceled by the r_0 -dependent term in $1/g_{11}$ [see Eqs. (21) and (23)]. The parameter r_0 thus drops out from Eq. (35), g_{11} being conveniently eliminated in favor of a_{11} . As far as Eq. (36) is concerned, one can just substitute the interaction term $g_{12}\delta_{r_0}(\sqrt{3}x/2)$ by the Bethe-Peierls boundary conditions at $x \rightarrow 0$

$$\phi(x) \propto |x| - 2a_{12}/\sqrt{3}, \quad D = 1, \quad (47)$$

$$\phi(x) \propto \ln(\sqrt{3}x/2a_{12}), \quad D = 2, \quad (48)$$

$$\phi(x) \propto 1 - 2a_{12}/\sqrt{3}x, \quad D = 3. \quad (49)$$

In other words, Eq. (36) is equivalent to

$$-\nabla_{\mathbf{x}}^2 \phi(\mathbf{x}) = -\sqrt{2/R_e^D} f(\mathbf{x}) \quad (50)$$

supplemented by the boundary conditions (47)-(49).

From now on, for brevity, we choose to measure all distances in units of R_e . The function $\tilde{f}(0)$ then depends on a_{11} and a_{12} (measured in units of R_e) and its dimension is clear from Eq. (40).

The idea of solving Eqs. (35) and (47)-(50) is to eliminate ϕ by inverting the Laplacian in Eq. (50) and then deal with a single integral equation for f . We perform this procedure in momentum space [the Fourier transform is defined by $\tilde{F}(p) = \int_{\mathbf{x}} F(x)e^{-i\mathbf{p}\mathbf{x}}$] where Eq. (50) formally transforms into $p^2\tilde{\phi}(p) = -\sqrt{2}\tilde{f}(p)$. Note, however, that we can always add to $\phi(\mathbf{x})$ a general solution of the Laplace equation $-\nabla_{\mathbf{x}}^2 \phi = 0$, possibly singular at the origin. The solution of Eq. (50) in momentum space is thus $-\sqrt{2}\tilde{f}(p)/p^2$ plus any linear combination of $\delta(\mathbf{p})$ and $1/p^2$. The freedom of choosing the corresponding coefficients is removed by Eq. (35) and the boundary conditions (47)-(49). The passage to momentum space in Eq. (35) is realized by rewriting the Fourier-space version of the operator

$$(\hat{L} + 1/g_{11})\tilde{f}(p) = \left(\frac{2}{\sqrt{3}}\right)^{D-2} \sum_{\pm} \int \frac{\tilde{f}(q)}{p^2 \pm \mathbf{p}q + q^2} \frac{d^D q}{(2\pi)^D} + \tilde{f}(p) \times \begin{cases} 1/2|p| - a_{11}/2, & D = 1, \\ -(1/2\pi)\ln(pa_{11}e^\gamma/2), & D = 2, \\ -p/4\pi + 1/4\pi a_{11}, & D = 3. \end{cases} \quad (51)$$

We now proceed to reformulating the boundary conditions (47)-(49) in momentum space. To this end let us first study the large- x behavior of $\phi(x)$ and $f(x)$ and check that these functions indeed possess well-defined Fourier transforms. When two atoms are far away from the third one (large x), the function ϕ is approximately proportional to Ψ due to Eq. (12), which is equivalent to having small f in Eq. (32). Thus, the large- x asymptotic behavior of $\phi(x)$ is given by Eq. (40) and, by calculating the second derivative of these asymptotes and using Eq. (50), we obtain the large- x scaling $f(x) \propto x^{-2D}$. We conclude that the passage to momentum representation is straightforward for $D > 1$ where $f(x)$ and $\phi(x)$ are well behaved. By contrast, in one dimension $\phi(x) \propto \ln|x|$ should be understood in the generalized sense by using a limit of a series of Fourier-transformable functions. In particular, we can use the relation $K_0(\sqrt{\epsilon}|x|) \approx -\ln \frac{\sqrt{\epsilon}|x|e^\gamma}{2}$ valid for small $\epsilon > 0$ and define a generalized Fourier transform of $\ln|x|$ as

$$-\frac{\pi}{|p|} = \lim_{\epsilon \rightarrow +0} \left[-\frac{\pi}{\sqrt{p^2 + \epsilon}} - 2\pi\delta(p) \ln \frac{\sqrt{\epsilon}e^\gamma}{2} \right]. \quad (52)$$

An immediate application of this formalism is the reformulation of the Bethe-Peierls boundary condition (47) in momentum space. Namely, for small x we have

$$\phi(x) = \int \tilde{\phi}(p) \frac{dp}{2\pi} - \frac{|x|}{2} \lim_{p \rightarrow \infty} p^2 \tilde{\phi}(p) + o(x), \quad (53)$$

where the integral is convergent, the singularity $\tilde{\phi}(p) \propto 1/|p|$ being understood in the sense of Eq. (52). Comparing Eq. (53) with (47) and denoting $C = \lim_{p \rightarrow \infty} p^2 \tilde{\phi}(p)$ gives us the Bethe-Peierls boundary condition in momentum space

$$\int \frac{\tilde{\phi}(p)}{C} \frac{dp}{2\pi} = \frac{a_{12}}{\sqrt{3}}. \quad (54)$$

Repeating the same procedure in two dimensions Eq. (48) transforms into

$$\int \left[\frac{\tilde{\phi}(p)}{C} - \frac{1}{p^2 + \sigma} \right] \frac{d^2 p}{(2\pi)^2} = \frac{1}{2\pi} \ln \frac{a_{12}\sqrt{\sigma}e^\gamma}{\sqrt{3}}, \quad (55)$$

where σ is any positive number. In the case $D = 3$, Eq. (49) becomes

$$\int \left[\frac{\tilde{\phi}(p)}{C} - \frac{1}{p^2} \right] \frac{d^3 p}{(2\pi)^3} = -\frac{\sqrt{3}}{8\pi a_{12}}. \quad (56)$$

The task of reformulating our problem in momentum space is thus over.

We now write the solution of Eq. (50) in the form

$$\tilde{\phi}(p) = \sqrt{2}(2\pi)^D \delta(\mathbf{p}) + \frac{C - \sqrt{2}\tilde{f}(p)}{p^2}. \quad (57)$$

Equation (57) is consistent with the definition of C (which is still unknown) and the coefficient in front of $\delta(\mathbf{p})$ is dictated by Eq. (35) and by the fact that the operator (51) does not give rise to a delta function. We now eliminate $\tilde{\phi}(p)$ by substituting Eq. (57) into Eqs. (35) and (54)-(56) and after simple manipulations we obtain the following results.

A. One dimension

In one dimension we arrive at

$$\tilde{f}(0) = \frac{1}{a_{12}/\sqrt{3} + I^{(1)}(a_{11})}, \quad (58)$$

where the function $I^{(1)}(a_{11}) = \int \frac{\chi(p)-1}{p^2} \frac{dp}{2\pi}$ is defined through the solution of

$$\frac{\sqrt{3}}{2} \sum_{\pm} \int \frac{\chi(q)}{p^2 \pm pq + q^2} \frac{dq}{2\pi} + \left(\frac{1}{2|p|} + \frac{1}{p^2} - \frac{a_{11}}{2} \right) \chi(p) = \frac{1}{p^2}, \quad (59)$$

$C = \sqrt{2}\tilde{f}(0)$, and $\tilde{f}(p) = \tilde{f}(0)\chi(p)$. Substituting Eq. (58) into Eq. (41) a_3 factorizes into (we restore the dimensions here)

$$a_3 = R_e \exp\left(\frac{2\pi}{3\sqrt{3}} \frac{a_{12}}{R_e}\right) \exp\left[\frac{2\pi}{3} I^{(1)}\left(\frac{a_{11}}{R_e}\right)\right], \quad (60)$$

consistent with Eq. (46) in the limit of small R_e/a_{12} .

Let us now discuss the function $I^{(1)}$. For large a_{11} (weak atom-atom interaction) this function can be expanded in powers of $\sqrt{-1/a_{11}}$. In order to see this we rescale the momentum $p = \sqrt{-1/a_{11}}z$ and rewrite Eq. (59) in the form

$$\chi(z) = \frac{1}{1 + z^2/2} - \frac{1}{\sqrt{-a_{11}}} \frac{z^2}{1 + z^2/2} \left[\frac{\sqrt{3}}{2} \sum_{\pm} \int \frac{\chi(y)}{z^2 \pm yz + y^2} \frac{dy}{2\pi} + \frac{\chi(z)}{2|z|} \right], \quad (61)$$

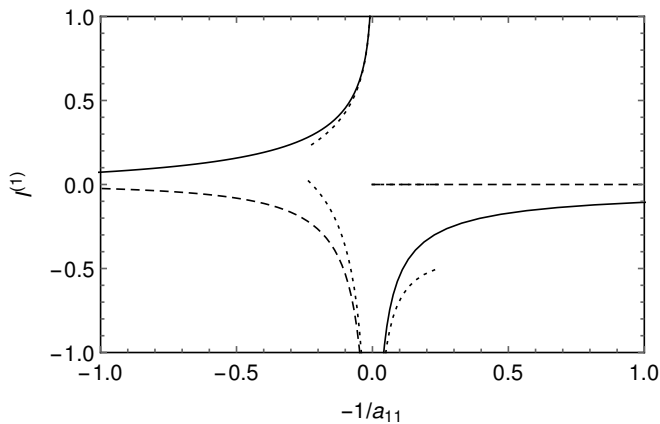


FIG. 1: Functions $\text{Re}I^{(1)}$ (solid) and $\text{Im}I^{(1)}$ (dashed) characterizing the dependence of the effective three-body interaction on a_{11} in one dimension [see Eqs. (58) and (40)]. a_{11} is measured in units of R_e . The dotted curves correspond to the large- a_{11} asymptote [Eq. (62)]. For $a_{11} \rightarrow \pm 0$ one has $I^{(1)} \approx -0.03$.

which we then solve iteratively. In particular, the first iteration gives $\chi(z) = 1/(1+z^2/2)$ and provides the leading order term $I^{(1)} \approx -\sqrt{-a_{11}/8}$. The second iteration results in

$$I^{(1)} = -\sqrt{-\frac{a_{11}}{8}} + \frac{9 + 5\sqrt{3}\pi + 27\ln(-a_{11}e^{-2\gamma}/2)}{36\pi} + o(1). \quad (62)$$

The solid and dashed lines in Fig. 1 show, respectively, the real and imaginary parts of $I^{(1)}$ as a function of $-1/a_{11}$ ($= g_{11}/2$) obtained numerically. The dotted lines indicate the real and imaginary parts of the large- a_{11} asymptote (62).

For negative a_{11} the solution is real and $\text{Im}I^{(1)} \equiv 0$. By contrast, for $a_{11} > 0$ the function $\chi(p)$ is characterized by simple poles at $p = \pm(\kappa + i0)$, where $\kappa > 0$ is defined by Eq. (24) [this is also the point where the term in round brackets in Eq. (59) vanishes]. These poles correspond to the three-body recombination to a dimer state, which, as found in Sec. III, exists only for positive a_{11} . One sees that $I^{(1)}$ and, therefore, $\tilde{f}(0)$ become complex reflecting the three-body loss. Technically, as one passes from positive to negative $-1/a_{11}$, the choice of the correct branch of the square root and logarithm in Eq. (62) is ensured by keeping $-1/a_{11}$ just below the real axis.

B. Two dimensions

The solution in the two-dimensional case can be written as

$$\tilde{f}(0) = \frac{2\pi}{\ln(a_{12}e^\gamma/\sqrt{3}) + 2\pi I^{(2)}(a_{11})}, \quad (63)$$

where $I^{(2)}(a_{11}) = \int \frac{\chi(p)-1/(p^2+1)}{p^2} \frac{d^2p}{(2\pi)^2}$ and χ satisfies

$$\sum_{\pm} \int \frac{\chi(q)}{p^2 \pm \mathbf{p}\mathbf{q} + q^2} \frac{d^2q}{(2\pi)^2} + \left(\frac{1}{p^2} - \frac{1}{2\pi} \ln \frac{a_{11}pe^\gamma}{2} \right) \chi(p) = \frac{1}{p^2}. \quad (64)$$

The three-body scattering surface is proportional to $\tilde{f}(0)$ [see Eq. (42)] and the mean-field result (5) is recovered for weak attractive or repulsive atom-dimer interactions (small or large a_{12}). As in the one-dimensional case we see that the dependence on a_{12} is analytic and for the complete solution of the problem one needs to know only $I^{(2)}(a_{11})$.

For a weak atom-atom background interaction (small or large a_{11}), introducing the small parameter $\lambda = 1/\ln(1/a_{11})$, we can proceed iteratively in exactly the same manner as in the one-dimensional case. Namely, using the momentum rescaling $p = \sqrt{\lambda}z$ one can see that to the leading order $\chi(z) \approx 1/(1+z^2/2\pi)$ and after two iterations we have

$$I^{(2)} = \frac{\ln(2\pi\lambda)}{4\pi} + \lambda \frac{\ln(C\lambda)}{8\pi} + o(\lambda), \quad (65)$$

where $C \approx 0.013$.

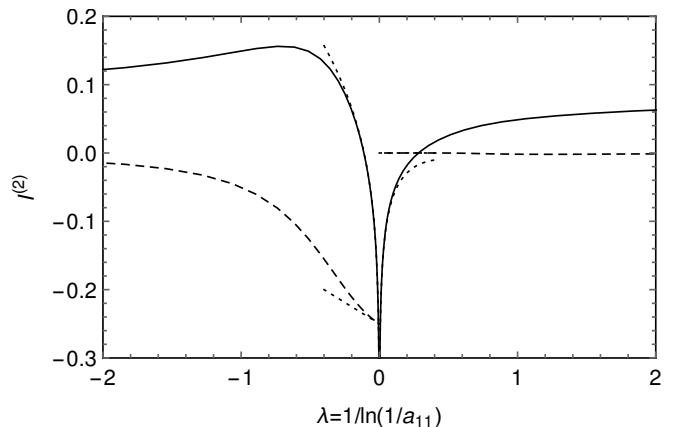


FIG. 2: Real and imaginary parts of $I^{(2)}$ in the two-dimensional case. We use the same notations as in Fig. 1.

In Fig. 2 we plot the real (solid) and imaginary (dashed) parts of $I^{(2)}$ versus λ together with the asymptote (65) (dotted). In the two-dimensional case $\text{Im}I^{(2)}$ is always finite since there is always a dimer bound state available for the recombination (see Sec. III). However, for small positive λ the dimer is exponentially deep and small (its energy is proportional to $1/a_{11}^2 = e^{-1/\lambda}$) so that the recombination in this limit is not captured by the power expansion Eq. (65).

Note that for small λ the characteristic momentum involved in the solution $\chi(p)$ is $\sqrt{\lambda}$. Therefore, the asymptotic expansion (65) is also valid if, instead of the zero-range atom-atom interaction, we have a

potential of a finite but sufficiently small range $\ll 1/\sqrt{\lambda} = \sqrt{|\ln(1/a_{11})|}$, characterized by the same scattering length a_{11} . In particular, one can have a purely repulsive potential which does not lead to a dimer state in our problem.

C. Three dimensions

In three dimensions we have

$$\tilde{f}(0) = \frac{1}{-\sqrt{3}/8\pi a_{12} + I^{(3)}(a_{11})}, \quad (66)$$

where $I^{(3)}(a_{11}) = \int \frac{\chi(p)}{p^2} \frac{d^3p}{(2\pi)^3}$ with χ satisfying

$$\frac{2}{\sqrt{3}} \sum_{\pm} \int \frac{\chi(q)}{p^2 \pm \mathbf{p} \cdot \mathbf{q} + q^2} \frac{d^3q}{(2\pi)^3} + \left(\frac{1}{p^2} - \frac{p}{4\pi} + \frac{1}{4\pi a_{11}} \right) \chi(p) = \frac{1}{p^2}. \quad (67)$$

Here we also manage to separate the dependencies on the atom-dimer and atom-atom interactions. The mean-field solution (5) is retrieved for $a_{12} \rightarrow 0$. Calculating $I^{(3)}$ is, however, more subtle than in the low-dimensional cases. Indeed, small hyperradii effectively correspond to high collision momenta and energies where the two-body scattering length is approximated by its background value a_{11} . Thus, at $p \ll a_{11}$ we deal with the Efimovian three-boson system which requires a three-body parameter or a cutoff momentum. Mathematically, this can be seen from Eq. (67) at momenta $p \gg 1/a_{11}$, where the dominant terms are the integral and $-p\chi(p)/4\pi$. The corresponding large-momentum behavior of $\chi(p)$ is a linear combination of Efimov waves $p^{\pm i s_0 - 2}$ with $s_0 \approx 1.00624$ [43]. The coefficients in this linear combination are fixed by introducing an external (three-body) parameter, phase, or momentum. Namely, one can set

$$\chi \propto \frac{\sin[s_0 \ln(p/p_0)]}{p^2} \quad (68)$$

as the asymptotic boundary condition for $p \gg 1/a_{11}$. Accordingly, the quantity $I^{(3)}$ is, in fact, a function of a_{11} and the three-body parameter p_0 . However, for small a_{11} the leading-order contribution to $I^{(3)}$ is universal, i.e., independent of p_0 . Indeed, for small a_{11} and momenta $p \ll 1/|a_{11}|$ Eq. (67) reduces to $(1/p^2 + 1/4\pi a_{11})\chi(p) = 1/p^2$. The corresponding solution $\chi = 1/(1 + p^2/4\pi a_{11})$ is characterized by the typical momentum $\sqrt{a_{11}} \ll 1/a_{11}$ and leads to

$$I^{(3)} \approx \sqrt{a_{11}/4\pi}. \quad (69)$$

In order to estimate the next-order term we match $\chi(p)$ with the Efimov wave (68) at momentum $p \sim 1/|a_{11}|$ obtaining a contribution to $I^{(3)}$ of the order of a_{11}^2 .

It makes sense to study the case of larger a_{11} ($\gtrsim R_e$) within our zero-range model, if we deal with a zero crossing near a narrow Feshbach resonance (large R_e) which,

in turn, lies in the vicinity of a broader Feshbach resonance (large a_{11}). At the same time it is interesting to have a significant atom-dimer interaction (large a_{12}) such that the two terms in the denominator of Eq. (66) are comparable. Then, in order to find the effective three-body force we also need to know the three-body and inelasticity parameters (or, equivalently, the real and imaginary parts of p_0), which could be known from the Efimov loss spectroscopy near the broad resonance. Given the large number of parameters in this problem we just give a prescription for calculating $I^{(3)}$. Namely, one has to solve Eq. (67) with the boundary condition (68) at $p \rightarrow \infty$ also requiring $\chi \propto 1/(p - \kappa - i0)$ near the pole given by Eq. (26).

V. DISCUSSION AND CONCLUSIONS

In this article we have expanded the idea that the bosonic model with a Feshbach-type atom-dimer conversion (1) near a two-body zero crossing can be reduced to a purely atomic model with an effective three-body interaction, which strongly depends on the atom-dimer conversion amplitude. As a particular example, we show that this mechanism of generating three-body forces can be used for stabilizing supersolid phases of two-dimensional dipoles.

Sections III and IV have been devoted to constructing a zero-range regularized version of the model (1) with a minimal set of parameters (a_{11} , a_{12} , and R_e). We have solved this model nonperturbatively in the two-body and three-body cases in all dimensions at the two-body zero crossing. Formulas (58), (63), and (66) give analytic dependencies of the three-body scattering amplitude on a_{12} in different dimensions. The dependence on a_{11} is found numerically and also analytically for weak atom-atom background interactions. In the three-dimensional case, our three-body zero-range model is Efimovian and requires an additional three-body parameter. We find, however, that for small $|a_{11}|/R_e$, effects associated with the Efimov physics are subleading.

These results show that for comparable and weak atom-dimer and atom-atom interactions (characterized by g_{12} and g_{11} , respectively), the three-body interaction is mostly influenced by g_{12} , consistent with the mean-field result (5). However, the convergence is not always uniform. For example, in the two-dimensional case, one can simultaneously decrease g_{12} and g_{11} , keeping both terms in the denominator of Eq. (63) comparable to (or even canceling) each other (resulting in a diverging three-body scattering surface). In the same spirit, we can use the nonperturbative three-dimensional formula Eq. (66) and predict a three-body resonance at $\sqrt{3}R_e/8\pi a_{12} \approx \sqrt{a_{11}/4\pi R_e} \ll 1$.

Inelastic three-body events manifest themselves through the appearance of an imaginary part of $\tilde{f}(0)$, which, in turn, comes from the complex $I^{(D)}$ or complex atom-dimer scattering length a_{12} . The former reflects

the three-body recombination to a dimer state and the latter the relaxation process in collisions of atoms with closed-channel dimers.

Several proposals on how to observe elastic three-body interactions experimentally are based on the following ideas. A repulsive three-body force could stabilize a system with attractive two-body interactions and make it self-trapped [16]. The structure and energies of few-body bound states, detectable spectroscopically, are also influenced by these forces [22, 24–26]. Collective-mode frequency shifts in a trapped gas could be another experimentally observable signature of three-body interactions

[32].

Acknowledgements

The research leading to these results received funding from the European Research Council (FP7/2007–2013 Grant Agreement No. 341197) and we acknowledge support from ANR grant Droplets No. ANR-19-CE30-0003-02.

-
- [1] H. Kadau, M. Schmitt, M. Wenzel, C. Wink, T. Maier, I. Ferrier-Barbut, and T. Pfau, Observing the Rosensweig instability of a quantum ferrofluid, *Nature (London)* **530**, 194 (2016).
 - [2] M. Schmitt, M. Wenzel, F. Böttcher, I. Ferrier-Barbut, and T. Pfau, Self-bound droplets of a dilute magnetic quantum liquid, *Nature (London)* **539**, 259 (2016).
 - [3] I. Ferrier-Barbut, H. Kadau, M. Schmitt, M. Wenzel, and T. Pfau, Observation of Quantum Droplets in a Strongly Dipolar Bose Gas, *Phys. Rev. Lett.* **116**, 215301 (2016).
 - [4] L. Chomaz, S. Baier, D. Petter, M. J. Mark, F. Wächtler, L. Santos, and F. Ferlaino, Quantum-Fluctuation-Driven Crossover from a Dilute Bose-Einstein Condensate to a Macrodroplet in a Dipolar Quantum Fluid, *Phys. Rev. X* **6**, 041039 (2016).
 - [5] C. R. Cabrera, L. Tanzi, J. Sanz, B. Naylor, P. Thomas, P. Cheiney, and L. Tarruell, Quantum liquid droplets in a mixture of Bose-Einstein condensates, *Science* **359**, 301 (2017).
 - [6] P. Cheiney, C. R. Cabrera, J. Sanz, B. Naylor, L. Tanzi, and L. Tarruell, Bright Soliton to Quantum Droplet Transition in a Mixture of Bose-Einstein Condensates, *Phys. Rev. Lett.* **120**, 135301 (2018).
 - [7] G. Semeghini, G. Ferioli, L. Masi, C. Mazzinghi, L. Wolswijk, F. Minardi, M. Modugno, G. Modugno, M. Inguscio, and M. Fattori, Self-Bound Quantum Droplets of Atomic Mixtures in Free Space, *Phys. Rev. Lett.* **120**, 235301 (2018).
 - [8] D. S. Petrov, Quantum mechanical stabilization of a collapsing Bose-Bose mixture, *Phys. Rev. Lett.* **115**, 155302 (2015).
 - [9] F. Wächtler and L. Santos, Quantum filaments in dipolar Bose-Einstein condensates, *Phys. Rev. A* **93**, 061603(R) (2016).
 - [10] R. N. Bisset, R. M. Wilson, D. Baillie, and P. B. Blakie, Ground-state phase diagram of a dipolar condensate with quantum fluctuations, *Phys. Rev. A* **94**, 033619 (2016).
 - [11] L. Tanzi, E. Lucioni, F. Famà, J. Catani, A. Fioretti, C. Gabanini, R. N. Bisset, L. Santos, and G. Modugno, Observation of a Dipolar Quantum Gas with Metastable Supersolid Properties, *Phys. Rev. Lett.* **122**, 130405 (2019).
 - [12] L. Chomaz, D. Petter, P. Ilzhöfer, G. Natale, A. Trautmann, C. Politi, G. Durastante, R. M. W. van Bijnen, A. Patscheider, M. Sohmen, M. J. Mark, and F. Ferlaino, Long-Lived and Transient Supersolid Behaviors in Dipolar Quantum Gases, *Phys. Rev. X* **9**, 021012 (2019).
 - [13] F. Böttcher, J.-N. Schmidt, M. Wenzel, J. Hertkorn, M. Guo, T. Langen, and T. Pfau, Transient Supersolid Properties in an Array of Dipolar Quantum Droplets, *Phys. Rev. X* **9**, 011051 (2019).
 - [14] L. Tanzi, S. M. Roccuzzo, E. Lucioni, F. Famà, A. Fioretti, C. Gabbanini, G. Modugno, A. Recati, and S. Stringari, Supersolid symmetry breaking from compressional oscillations in a dipolar quantum gas, *Nature (London)* (2019) doi:10.1038/s41586-019-1568-6.
 - [15] M. Guo, F. Böttcher, J. Hertkorn, J.-N. Schmidt, M. Wenzel, H.-P. Büchler, T. Langen, and T. Pfau, The low-energy Goldstone mode in a trapped dipolar supersolid, *Nature (London)* (2019) doi:10.1038/s41586-019-1569-5.
 - [16] A. Bulgac, Dilute Quantum Droplets, *Phys. Rev. Lett.* **89**, 050402 (2002).
 - [17] D. S. Petrov, Three-Body Interacting Bosons in Free Space, *Phys. Rev. Lett.* **112**, 103201 (2014).
 - [18] K.-T. Xi and H. Saito, Droplet formation in a Bose-Einstein condensate with strong dipole-dipole interaction, *Phys. Rev. A* **93**, 011604(R) (2016).
 - [19] R. N. Bisset and P. B. Blakie, Crystallization of a dilute atomic dipolar condensate, *Phys. Rev. A* **92**, 061603(R) (2015).
 - [20] Z.-K. Lu, Y. Li, D. S. Petrov, and G. V. Shlyapnikov, Stable dilute supersolid of two-dimensional dipolar bosons, *Phys. Rev. Lett.* **115**, 075303 (2015).
 - [21] A. Pricoupenko and D. S. Petrov, Dimer-dimer zero crossing and dilute dimerized liquid in a one-dimensional mixture, *Phys. Rev. A* **97**, 063616 (2018).
 - [22] Y. Sekino and Y. Nishida, Quantum droplet of one-dimensional bosons with a three-body attraction, *Phys. Rev. A* **97**, 011602(R) (2018).
 - [23] J. E. Drut, J. R. McKenney, W. S. Daza, C. L. Lin, and C. R. Ordóñez, Quantum Anomaly and Thermodynamics of One-Dimensional Fermions with Three-Body Interactions, *Phys. Rev. Lett.* **120**, 243002 (2018).
 - [24] Y. Nishida, Universal bound states of one-dimensional bosons with two- and three-body attractions, *Phys. Rev. A* **97**, 061603 (2018).
 - [25] L. Pricoupenko, Pure confinement-induced trimer in one-dimensional atomic waveguides, *Phys. Rev. A* **97**, 061604 (2018).
 - [26] G. Guizarro, A. Pricoupenko, G. E. Astrakharchik, J. Boronat, and D. S. Petrov, One-dimensional three-

- boson problem with two- and three-body interactions, Phys. Rev. A **97**, 061605(R) (2018).
- [27] L. Pricoupenko, Three-body pseudopotential for atoms confined in one dimension, Phys. Rev. A **99**, 012711 (2018).
 - [28] W. S. Daza, J. E. Drut, C. L. Lin, C. R. Ordóñez, A Quantum Field-Theoretical Perspective on Scale Anomalies in 1D systems with Three-Body Interactions, Mod. Phys. Lett. A **34**, 1950291 (2019).
 - [29] J. R. McKenney and J. E. Drut, Fermi-Fermi crossover in the ground state of one-dimensional few-body systems with anomalous three-body interactions, Phys. Rev. A **99**, 013615 (2019).
 - [30] V. Pastukhov, Ground-state properties of dilute one-dimensional Bose gas with three-body repulsion, Phys. Lett. A **383**, 894 (2019).
 - [31] M. Valiente, Three-body repulsive forces among identical bosons in one dimension, Phys. Rev. A **100**, 013614 (2019).
 - [32] M. Valiente and V. Pastukhov, Anomalous frequency shifts in a one-dimensional trapped Bose gas, Phys. Rev. A **99**, 053607 (2019).
 - [33] L. Radzihovsky, P. B. Weichman, and J. I. Park, Superfluidity and phase transitions in a resonant Bose gas, Ann. Phys. **323**, 2376 (2008).
 - [34] M. A. Baranov, A. Micheli, S. Ronen, and P. Zoller, Bilayer superfluidity of fermionic polar molecules: Many-body effects, Phys. Rev. A **83**, 043602 (2011).
 - [35] Z. Shotan, O. Machtey, S. Kokkelmans, and L. Khaykovich, Three-Body Recombination at Vanishing Scattering Lengths in an Ultracold Bose Gas, Phys. Rev. Lett. **113**, 053202 (2014).
 - [36] G. Quémener and J. L. Bohn, Electric field suppression of ultracold confined chemical reactions, Phys. Rev. A **81**, 060701(R) (2010).
 - [37] A. Micheli, Z. Idziaszek, G. Pupillo, M. A. Baranov, P. Zoller, and P. S. Julienne, Universal Rates for Reactive Ultracold Polar Molecules in Reduced Dimensions, Phys. Rev. Lett. **105**, 073202 (2010).
 - [38] A. Frisch, M. Mark, K. Aikawa, S. Baier, R. Grimm, A. Petrov, S. Kotochigova, G. Quémener, M. Lepers, O. Dulieu, and F. Ferlaino, Ultracold Dipolar Molecules Composed of Strongly Magnetic Atoms, Phys. Rev. Lett. **115**, 203201 (2015).
 - [39] R. Stock, A. Silberfarb, E. L. Bolda, and I. H. Deutsch, Generalized Pseudopotentials for Higher Partial Wave Scattering, Phys. Rev. Lett. **94**, 023202 (2005).
 - [40] K. Kanjilal and D. Blume, Coupled-channel pseudopotential description of the Feshbach resonance in two dimensions, Phys. Rev. A **73**, 060701(R) (2006).
 - [41] D. S. Petrov, in *Proceedings of the Les Houches Summer Schools, Session 94*, edited by C. Salomon, G. V. Shlyapnikov, and L. F. Cugliandolo (Oxford University Press, Oxford, England, 2013).
 - [42] The prefactor $\sqrt{3}/2$ here [and also in Eqs. (36), (47-49)] comes from our definition of the Jacobi coordinates (28), according to which the atom-dimer distance equals $\sqrt{3}x/2$.
 - [43] See, for example, page 359 in E. Braaten and H.-W. Hammer, Universality in few-body systems with large scattering length, Phys. Rep. **428**, 259 (2006).